Processing and Application of Ceramics 12 [2] (2018) 123–128
https://doi.org/10.2298/PAC1802123K

Processing and mechanical characterization of Al_2O_3/Ni and Al_2O_3/Co composites by pressureless sintering of nanocomposite powders

Betül Kafkaslioğlu Yildiz*, Hüseyin Yilmaz, Yahya Kemal Tür

Department of Materials Science and Engineering, Gebze Technical University, 41400 Gebze, Kocaeli, Turkey

Received 25 December 2017; Received in revised form 1 March 2018; Accepted 12 May 2018

Abstract

Al_2O_3/Ni and Al_2O_3/Co nanopowder mixtures (with 3 vol.% of metallic phase) were synthesized by heterogeneous precipitation method. In order to increase the green strength, polypropylene carbonate (PPC) was used as a binder while preparing green compacts. Uniaxially pressed powder mixtures were sintered at 1550 °C for 2 h in a reducing atmosphere. The effects of Ni and Co nanophases on the microstructure and mechanical properties of Al_2O_3 ceramics were studied by X-ray diffraction, scanning electron microscopy, Vickers indentation technique and three-point bending tests. The metallic phase hindered the densification of alumina matrix, yet hardness values of Al_2O_3, Al_2O_3/Ni, and Al_2O_3/Co composites were comparable. Vickers fracture toughness results indicate that the composites have higher fracture toughness, but the characteristic flexural strength and Weibull modulus are higher for the pure Al_2O_3.

Keywords: *alumina, composites, sintering, toughness, toughening, Weibull strength*

I. Introduction

Al_2O_3 is one of the most used advanced ceramic materials due to its superior properties, such as high compressive strength, high hardness, and high thermal stability as compared to the other structural ceramics [1]. However, the use of Al_2O_3 for structural applications is frequently restricted by its low fracture toughness and low tensile strength [2–4]. Al_2O_3 based ceramic matrix composites incorporated with ductile metal particles have been widely investigated to improve the mechanical properties [5]. Especially, Al_2O_3/metal nanocomposites are of great interest because of enhancement in both hardness and strength together with a slight increase in toughness [6,7]. The particular case of the Al_2O_3/Ni system has been extensively studied for a long time [3,7,8]. Al_2O_3/Co composites are considered an alternative to the Al_2O_3/Ni system, due to the superior properties of cobalt, like high melting temperature (1495 °C) compared with the nickel systems and good biocompatibility [9–11]. The solution chemistry routes, in which metal nitrates are used as metal precursors for the production of ceramic/metal nanocomposites, could be advantageous to provide a fine-scale homogeneity [7,12]. The heterogeneous precipitation method provides not only nanosized metal powders, but also a homogeneous metal particle dispersion [8,12].

It is known that the processing route, the employed pressure, sintering temperature and time besides other processing parameters may all affect the defect size in ceramic materials. In turn, the strength of ceramic materials depends on the size of the defects that varies from specimen to specimen. Therefore, the strength of ceramics is statistical in nature. Weibull used a statistical technique to analyze the reliability of ceramics. Reliability can be defined as the probability of survival at a given stress level. Weibull statistics is based on the weakest link theory, which means that the most serious flaw in the material will control the strength, like a chain breaking if its weakest link fails [13,14]. Two-parameter Weibull distribution, which defines the reliability at a given stress level in terms of the characteristic flexural strength, σ_0, and the Weibull modulus, m, was used to analyze the strength of the specimens in the present study.

In this work, Al_2O_3/Ni and Al_2O_3/Co nanopowder mixtures (with 3 vol.% of metallic phase) were obtained

* Corresponding author: tel: +90 2626052689,
fax: +90 2626530675, e-mail: *bkafkaslioglu@gtu.edu.tr*

by the heterogeneous precipitation method as it can provide homogeneous metal particle dispersion [8,12]. In ceramic processing, binders are often used to improve the strength of the green compacts and sometimes the relative density [15]. There are various organic binders which are either soluble in water or organic solvents, like PVA (polyvinylalcohol) and PEG (polyethyleneglycol), but polypropylene carbonate (PPC) was selected because it burns out completely during the sintering cycle in reducing atmosphere conditions [16]. The effects of Ni and Co particles on the microstructure and mechanical properties of sintered Al_2O_3 ceramics was investigated.

II. Experimental procedure

The starting materials were α-Al_2O_3 powder with average diameter of 0.60 μm (Almatis Calcined Al_2O_3, Germany), nickel nitrate hexahydrate ($Ni(NO_3)_2 \cdot 6\,H_2O$, BDH Chemicals Ltd., Poole, England, 98% purity), cobalt nitrate hexahydrate ($CoN_2O_6 \cdot 6\,H_2O$, Sigma-Aldrich, 98% purity), ammonium bicarbonate (NH_4HCO_3, Sigma Aldrich, 99% purity), and polyacrylic acid as dispersant (Darvan 821A from MSE Tech Co. Ltd., Turkey). Finally, polypropylene carbonate (PPC) (QPAC 40, Empower Materials, USA) was preferred as a binder.

Al_2O_3 powder with an appropriate amount of metal nitrate hexahydrate that provides 3 vol.% metal content in the final composite, and 0.5 wt.% (equivalent to Al_2O_3 weight) polyacrylic acid were mixed in distilled water and ball milled for 24 hours with alumina balls (ball : Al_2O_3 powder ratio of 10 : 1 by weight). 1.0 M aqueous solution of NH_4HCO_3 (the precipitation agent) was added dropwise to the prepared slurry under vigorous stirring. The reactions were given by the following equations [8,12,17]:

$$3\,Ni^{2+} + 6\,HCO_3^{1-} + H_2O \longrightarrow NiCO_3 \cdot 2\,Ni(OH)_2 \cdot 2\,H_2O\downarrow + \\ + 5\,CO_2\uparrow \quad (1)$$

$$3\,Co^{2+} + 6\,HCO_3^{1-} + H_2O \longrightarrow CoCO_3 \cdot 2\,Co(OH)_2 \cdot 2\,H_2O\downarrow + \\ + 5\,CO_2\uparrow \quad (2)$$

To guarantee the completion of above reactions during precipitation, an excess amount of NH_4HCO_3 was used and the pH value of the slurries was kept between 8–9. After precipitation, the slurries were filtered, washed with distilled water and ethanol. After drying in air for 24 h, the dried powders were first calcined in air at 500 °C for 2 h and then reduced in a 90% Ar/10% H_2 atmosphere at 700 °C/4 h for Ni and at 950 °C/2 h for Co [8,17] nanocomposite powder mixture. The reducing cycles were 5 °C/min for both calcination and reduction treatment and then cooled down to room temperature in the furnace. Following these heat treatments, metal coated Al_2O_3 composite powder could be obtained. The pure Al_2O_3 powder was prepared under the same conditions to compare the final properties with composites. The pure alumina powder and reduced powder mixtures were sieved down to 90 μm and pressed into a rectangular prism form in a 40 × 50 mm steel mould under the uniaxial pressure of 100 MPa. However, the pressed samples were cracked and broke up easily while removing from the mould. In order to increase the green strength, 3 wt.% and 2 wt.% PPC binders were added to the alumina and composite powders, respectively. A stock solution of PPC was prepared by dissolving it in acetone and acetone was allowed to evaporate from the powder mixture before sieving. Then the powders were dried and sieved again. The pressing procedure was repeated and the specimens in required form and strength could be obtained. All the specimens were pressureless sintered in a vertical tube furnace in reducing (90% Ar + 10% H_2) atmosphere. The specimens were heated to 350 °C at a heating rate of 2 °C/min and held for 1 h at this temperature for complete elimination of the binder. The samples were then heated to 1550 °C at a heating rate of 5 °C/min with 2 h dwell time. After sintering, the prismatic bars were cut from the pieces with 3 mm width, 2 mm thickness, and 40 mm length.

The phase analysis was carried out by X-ray diffractometry (XRD) at a scanning rate of 4°/min with a 2θ range from 10° to 70° by a Bruker® D8 Advance diffractometer and the bulk density of the sintered specimens was measured by the Archimedes' method. Scanning electron microscope (SEM, Philips XL 30 SFEG) was employed to characterize the microstructure of the samples. The samples were ground and polished to see the grains and metal phases clearly in SEM analysis and to eliminate the effect of surface flaws on mechanical properties. Also, thermal etching was done to reveal the grain boundaries at 1400 °C for 1 h under 90% Ar + 10% H_2 atmosphere. The alumina matrix grain size was measured by using SEM secondary electron mode micrographs with the linear intercept method where more than 100 intercepts are counted and averaged for each composition. Ni and Co particle sizes were estimated by averaging the particle sizes from five SEM backscattered electron mode micrographs of different locations at magnification of 10 000.

Hardness was measured by using an Instron® tester (Wolpert Testor 2100) equipped with a diamond pyramid Vickers indenter under 5 kg of the load with a dwell time of 10 s. The fracture toughness was calculated using the Vickers indentation technique in which 10 kg of the load was applied for 10 s and using the equation by Anstis [18]:

$$K_C = 0.016 \cdot \left(\frac{E}{H_V}\right)^{1/2} \cdot \frac{P}{c^{3/2}} \quad (3)$$

where P is the maximum loading force, c is the length from the centre of the contact to the end of the crack, E is the elastic modulus and H_V is Vickers hardness. The flexural strength was measured by 3-point bending test with a load span of 20 mm and a loading rate

of 0.2 mm/s; two-parameter Weibull analysis was employed to analyze measured flexural strength values.

III. Results and discussion

After calcination of the Al_2O_3-precipitated metal precursor powder mixture at 500 °C for 2 h in the air, the crystallization of discrete metal oxide phase occurred. By heat treatment at 700 °C/4 h and 950 °C/2 h in reducing atmosphere, metal oxide particles were all reduced to Ni and Co particles dispersed on the Al_2O_3 powder that was showed in XRD patterns in Fig. 1. The calcination and reduction parameters were determined according to results of Li *et al.* [8]. Li [8] and Kafkaslıoğlu [12] verified that the metal particles formed after heat treatments were nanosized by using transmission electron microscopy (TEM) and SEM micrographs, respectively. Figure 1 shows the XRD patterns of the Al_2O_3/Ni and Al_2O_3/Co composites (with 3 vol.% of metallic phase) after calcination, reducing and sintering. Only Ni and NiO or Co and CoO peaks are labeled for clarity, while not labeled peaks belong to α-Al_2O_3. When the patterns presented in Fig. 1a are analyzed, it can be seen that after reducing only Ni peaks are present and after sintering at 1550 °C, the peaks of Ni metal phase become more pronounced. This increase in peak intensity is attributed to the growth of metal phase from nano sizes (about 50 nm) to submicron sizes (from 100 nm to 1 μm). Figure 1b shows the XRD patterns of Al_2O_3/Co composites and similar to Ni containing composites, CoO peaks were replaced by Co peaks after reducing and the intensities of Co peaks increase after sintering at 1550 °C due to Co particle growth.

Cobalt displays a martensitic transformation from FCC to HCP at 417 °C during cooling; however, these two forms of cobalt usually coexist at room temperature and a martensitic transformation from FCC-Co to HCP-Co may contribute to the toughness of the material similar to the martensitic transformation of zirconia. Tai *et al.* [19] reported that in alumina reinforced by submicrometer Co particles, Co is mostly in FCC form and after polishing a fraction of the FCC particles transforms to HCP. In order to determine Co structure in sintered, polished and fractured specimens, 2θ between 40° and 50° has been carefully scanned and XRD pattern is investigated for main FCC peak (44.35°, JCPDS card no. 05-0727) and main HCP peak (47.57°, JCDPS card no 15-0806) [20]. On all three surfaces no indication of HCP peak is observed; therefore, transformation toughening is not expected.

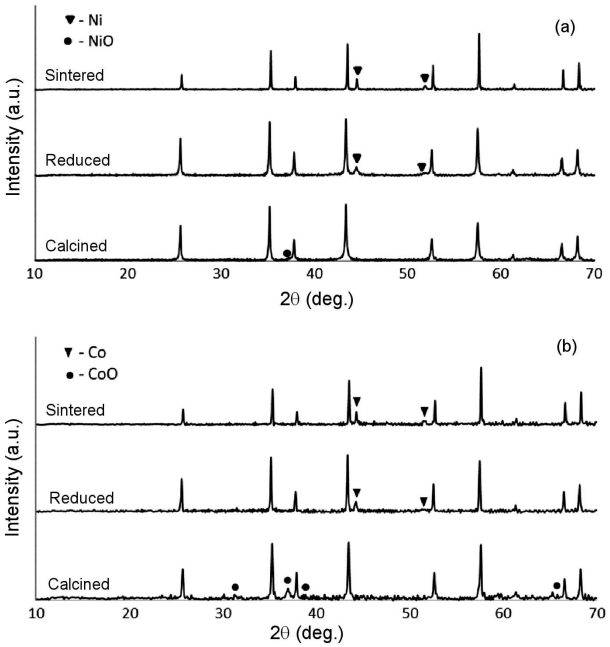

Figure 1. XRD patterns of a) Al_2O_3/Ni and b) Al_2O_3/Co composite after calcination, reduction, and sintering (not labelled peaks are Al_2O_3)

Theoretical densities of Al_2O_3/Ni and Al_2O_3/Co composites (with 3 vol.% of metallic phase) were calculated using the rule of mixtures and compared with the experimental results. As presented in Table 1, Al_2O_3/Ni and Al_2O_3/Co have comparable relative densities, which was lower than that of Al_2O_3. The relative density difference between composites and Al_2O_3 can also be seen from SEM micrographs given in Fig. 2. Even though the addition of PPC increased the green strength and the homogeneity of the specimens, densification of the composite specimens was below the pure Al_2O_3. The decrease in relative density, which is detrimental to mechanical properties of ceramic materials, could be attributed to poor wetting of alumina by the Ni and Co melts, which hinders the densification of Al_2O_3 [21].

Figure 2 shows SEM micrographs of thermally etched monolithic Al_2O_3 and the composite specimens in secondary electron mode. The metal particles that were located at the triple junctions and at the grain boundaries seem brighter and Al_2O_3 grains seem darker. In both composites, metal particles were found to be spherical and dispersed homogeneously throughout the matrix. Alumina grain sizes and metal particle sizes for monolithic Al_2O_3, Al_2O_3/Ni and Al_2O_3/Co composites are given in Table 1. The average alumina grain

Table 1. Relative density (ρ_r), alumina grain size (D_A), metal particle size (D_M), Vicker's indentation hardness (H_V), Vicker's fracture toughness (K_C), characteristic flexural strength (σ_0) and the Weibull modulus (m) of Al_2O_3, Al_2O_3/Ni and Al_2O_3/Co composites

Material	ρ_r [%TD]	D_A [μm]	D_M [μm]	H_V [GPa]	K_C [MPa·m$^{1/2}$]	σ_0 [MPa]	m
Al_2O_3	98.9 ± 0.2	~1.9	-	21.7 ± 1.3	3.68 ± 0.45	623	10.2
Al_2O_3/Ni	97.8 ± 0.3	~1.7	0.64 ± 0.12	21.6 ± 1.0	4.42 ± 0.67	550	6.6
Al_2O_3/Co	97.8 ± 0.3	~2.0	0.71 ± 0.22	21.9 ± 1.1	4.67 ± 0.96	588	7.8

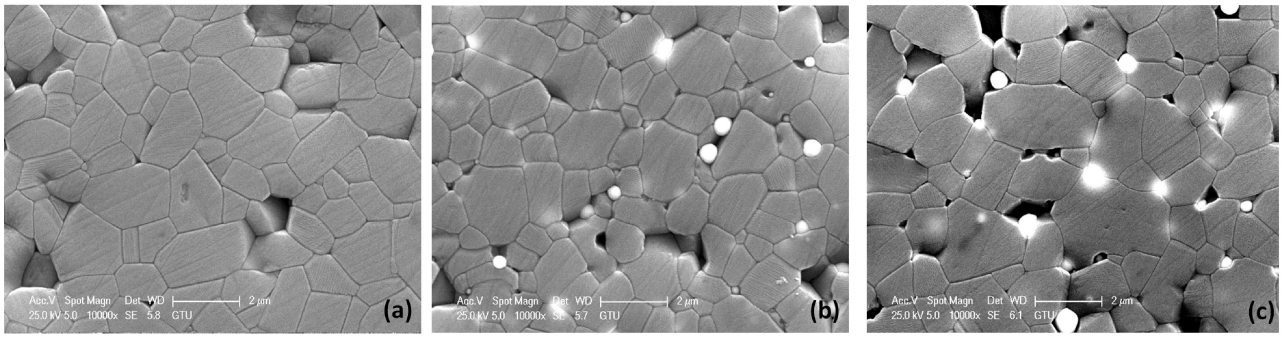

Figure 2. SEM micrographs of: a) Al_2O_3, b) Al_2O_3/Ni and c) Al_2O_3/Co specimens sintered at 1550 °C (metal particles are bright and Al_2O_3 matrix appears darker)

sizes of Al_2O_3, Al_2O_3/Ni and Al_2O_3/Co samples are 2.0 μm, 1.7 μm and 1.9 μm, respectively. It seems that the presence of Ni particles has a stronger influence on the growth of Al_2O_3 grains. Also, Ni and Co particle sizes in the composites were 0.64 ± 0.12 μm and 0.71 ± 0.22 μm, respectively; i.e. Co reinforced composites had slightly larger average size of metal particles. Even tough Co has a relatively higher melting temperature (1495 °C) compared to Ni melting temperature (1455 °C), it appears that at the sintering temperature of 1550 °C, Co particles have relatively higher mobility in alumina matrix which resulted in larger Al_2O_3 and Co particle sizes.

As seen from Table 1, Vickers hardness measurements show that the pure Al_2O_3 and the Al_2O_3/Ni and Al_2O_3/Co composites have similar hardness values. The soft character of metal phases would expect to decrease the hardness of the composite by the rule of mixtures. Also, lower relative densities of the composites should result in decreased hardness for these materials. On the other hand, the submicron size of metal particles inhibits the dislocation motion and increases the hardness of the metal phase and compensates for the decrease in hardness due to lower densities of the composites [12].

Fracture toughness values of Al_2O_3/Ni and Al_2O_3/Co composites are 4.4 ± 0.7 and 4.7 ± 0.9 MPa·m$^{1/2}$, respectively. In contrast with hardness measurements, indentation fracture toughness of the pure Al_2O_3 (3.7 ± 0.5 MPa·m$^{1/2}$) is lower than that of the composites. These values correspond to 19% and 27% increment in toughness, which are quite high considering only 3 vol.% metal particle phase is present. The mechanism for increasing the fracture toughness is believed to be a combination of the plastic deformation of the ductile phase ahead of the crack tip and the crack bridging at the wake of the crack preventing further opening of the crack [8]. It seems that addition of 3 vol.% of cobalt by the heterogeneous precipitation method is more effective to enhance the fracture toughness of the alumina matrix. SEM observations reveal that Co particles were larger compared to Ni particles and the enhanced fracture toughness is attributed to these larger ductile particles. Since HCP-Co was not detected in XRD analysis, FCC to HCP phase transformation of Co particles was not considered to be a factor in toughening of the Al_2O_3/Co composite.

The strength of ceramic materials, σ_f, depends on the fracture toughness, K_C, and the defect size, a, of the material as given in Eq. 6 [22]:

$$\sigma_f = \frac{K_C}{Y \cdot \sqrt{\pi \cdot a}} \tag{4}$$

where Y is the stress intensity geometry factor. In order to increase the strength, higher fracture toughness and small defect size are desired. The strength of ceramics is statistical in nature and the Weibull distribution has been widely used to analyze the scatter in strengths [14]. The probability of failure in two parameters Weibull distribution is given by:

$$P_f(\sigma) = 1 - \exp\left[-\left(\frac{\sigma}{\sigma_0}\right)^m\right] \tag{5}$$

where P_f is the probability of failure, m is the Weibull modulus, σ_0 is the characteristic strength, and σ is the failure stress. The probability of failure, P_f, was calculated using the equation [23]:

$$P_{f,i} = \frac{i - 0.5}{n} \tag{6}$$

where n is the total number of the samples tested and i is the sample rank in ascending order of failure stress. In Eq. 5, $\sigma = \sigma_0$ corresponds to 0.632; that is, the stress at the 63.2% probability of failure gives the characteristic strength (σ_0). The Weibull modulus is estimated by plotting the $\ln(\sigma)$ vs $\ln(\ln(1/(1 - P_f)))$ data, the slope of the linear regression line gives the Weibull modulus, m.

Figure 3 shows the Weibull plots, i.e. flexural strength versus Weibull percentile for the pure Al_2O_3 and composites. Even though the pure Al_2O_3 has a lower toughness compared to the composites, it has the highest characteristic flexural strength and the highest Weibull modulus. Using K_C and σ_0 values from Table 1 and assuming a semi-circular surface crack under uniform loading, crack sizes corresponding to the characteristic strength are evaluated to be 22 μm for Al_2O_3 and 40 μm for both Al_2O_3/Ni and Al_2O_3/Co composites. In other words, in-

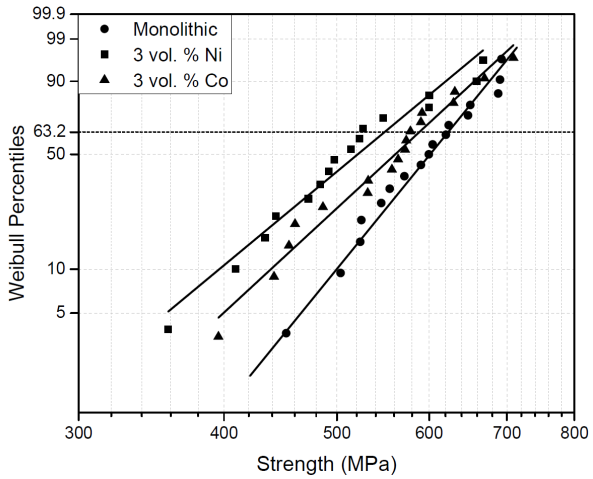

Figure 3. Weibull plots of Al_2O_3, Al_2O_3/Ni and Al_2O_3/Co specimens

trinsic defect size of monolithic alumina is smaller than Ni and Co containing composites. It appears that Al_2O_3 has a smaller intrinsic defect size, almost half of the composites, due to its higher relative density. Consequently, the higher relative density of the alumina more than makes up for the lower toughness of the material and it has the highest flexural strength.

Not only a high characteristic strength but also a high Weibull modulus is desired from ceramic materials in order to attain high reliability of components and both of these can be achieved by eliminating large defects in the microstructure [24]. Monolithic Al_2O_3 with its highest relative density has the highest Weibull modulus, m = 10.2, whereas Al_2O_3/Ni and Al_2O_3/Co composites m values are lower, 6.6 and 7.8, respectively. It is concluded that even tough Ni and Co particles enhance fracture toughness of the composite material, in order to materialize this increase, composites with equal or higher densities than the pure Al_2O_3 must be prepared.

IV. Conclusions

Al_2O_3/Ni and Al_2O_3/Co powder mixtures with 3 vol.% metal contents were prepared successfully by the heterogeneous precipitation method. The addition of PPC increased the strength and homogeneity of the green specimens. For the specimens sintered at 1550 °C for 2 h in a reducing atmosphere, the highest density was observed for Al_2O_3, the metal phase addition decreased the densification. The addition of metal phase, specifically Co, increased the toughness of the composite material. However, due to smaller defect size accompanied with the higher densification, maximum Weibull strength and Weibull modulus values were still achieved in Al_2O_3. In order to exploit the toughening effect of the metal phase to achieve higher strengths, near full densification of the composites is required.

Acknowledgement: The support of GTU Scientific Research Council #2015-A-33 project is greatly appreciated.

References

1. Y.I. Lee, J.T Lee, Y.H. Choa, "Effects of Fe-Ni alloy nanoparticles on the mechanical properties and microstructures of Al_2O_3/Fe-Ni nanocomposites prepared by rapid sintering", *Ceram. Int.*, **38** [5] (2012) 4305–4312.
2. M. Uysal, R. Karslıoğlu, A. Alp, H. Akbulut, "The preparation of core-shell Al_2O_3/Ni composite powders by electroless plating", *Ceram. Int.*, **39** [5] (2013) 5485–5493.
3. T. Isobe, K. Daimon, K. Ito, T. Matsubara, Y. Hikichi, T. Ota, "Preparation and properties of Al_2O_3/Ni composite from $NiAl_2O_4$ spinel by in situ reaction sintering method", *Ceram. Int.*, **33** [7] (2007) 1211–1215.
4. H. Bian, Y. Yang, Y. Wang, W. Tian, H. Jiang, Z. Hu, W. Yu, "Effect of microstructure of composite powders on microstructure and properties of microwave sintered alumina matrix ceramics", *J. Mater. Sci. Technol.*, **29** [5] (2013) 429–433.
5. W.G. Fahrenholtz, D.T. Ellerby, R.E. Loehman, "Al_2O_3-Ni composites with high strength and fracture toughness", *J. Am. Ceram. Soc.*, **83** [5] (2000) 1279–80.
6. T. Rodriguez-Suarez, J.F. Bartolome, A. Smirnov, "Sliding wear behavior of alumina nickel nanocomposites processed by a conventional sintering route", *J. Eur. Ceram. Soc.*, **31** [8] (2011) 1389–1395.
7. R.Z. Chen, W.H. Tuan, "Pressureless sintering of Al_2O_3/Ni nanocomposites", *J. Eur. Ceram. Soc.*, **19** [4] (1999) 463–468.
8. G.J. Li, R.M. Ren, X.X. Huang, J.K. Guo, "Microstructure and mechanical properties of Al_2O_3/Ni composites", *Ceram. Int.*, **30** [6] (2004) 977–982.
9. D.S. Mao, J. Li, S.Y. Guo, "Study of abrasion behavior of an advanced Al_2O_3-TiC-Co ceramic", *Wear*, **209** [1-2] (1997)153–159.
10. B.T. Lee, K.H. Kim, A.H.M. Esfakur Rahman, H.Y. So, "Microstructures and mechanical properties of spark plasma sintered Al_2O_3-Co composites using electroless deposited Al_2O_3-Co powders", *Mater. Trans.*, **49** [6] (2008) 1451–1455.
11. D. Maruoka, T. Itaya, T. Misaki, M. Nanko, "Recovery of mechanical property on nano-Co particles dispersed Al_2O_3 via high-temperature oxidation", *Mater. Trans.*, **53** [10] (2012) 1816–1821.
12. B. Kafkaslıoğlu, Y.K. Tür, "Pressureless sintering of Al_2O_3/Ni nanocomposites produced by heterogeneous precipitation method with varying nickel contents", *Int. J. Refract. Met.*, **57** (2016) 139–144.
13. Y. Fu, Z. Tao, X. Hou, "Weibull distribution of the fracture strength of 99% alumina ceramic reshaped by cold isostatic pressing", *Ceram. Int.*, **40** [6] (2014) 7661–7667.
14. S. Wei, Z. Xie, W. Xue, Z. Yi, J. Chen, L. Cheng, "Strengthening mechanism of aluminum nitride ceramics from 293 to 77 K", *Mater. Lett.*, **119** (2014) 32–34.
15. C.A. Say, D.A. Earl, M.J. Thompson, "Optimization of the sintered density of aluminum oxide compacts", *Mater. Lett.*, **53** [4-5] (2002) 262–267.
16. V.G. Karayannis, A.K. Moutsatsou, "Synthesis and characterization of nickel-alumina composites from recycled nickel powder", *Adv. Mater. Sci. Eng.*, **2012** (2012) 395612.
17. X. Shi, Y. Pan, J. Guo, "Fabrication and magnetic properties of cobalt-dispersed-alumina composites", *Ceram. Int.*, **33** [8] (2007) 1509–1513.

18. G.R. Anstis, T. Chantikul, B.R. Lawn, D.B. Marshall, "A critical evaluation of indentation techniques for measuring fracture toughness: I, direct crack measurements", *J. Am. Ceram. Soc.*, **64** [9] (1981) 533–538.
19. W.P. Tai, T. Watanabe, "Preparation and mechanical properties of Al_2O_3 reinforced by submicron Co particles", *J. Mater. Sci.*, **33** [24] (1998) 5795–5801.
20. N.A.M. Barakat , B. Kim, S.J. Park, Y. Jo, M.H. Jung, H.Y. Kim, "Cobalt nanofibers encapsulated in a graphite shell by an electrospinning process", *J. Mater. Chem.*, **19** [39] (2009) 7371–7378.
21. M. Humenik, W.D. Kingery, "Metal-ceramic interactions: surface tension and wettability of metal-ceramic systems", *J. Am. Ceram. Soc.*, **37** [1] (1954) 18–23.
22. A.G. Evans, "Perspective on the development of high-toughness ceramics", *J. Am. Ceram. Soc.*, **73** [2] (1990) 187–206.
23. J. Zhang, D. Estévez, Y.Y. Zhaoet, L. Huo, C. Chang, X. Wang, R.W. Li, "Flexural strength and Weibull analysis of bulk metallic glasses", *J. Mater. Sci. Technol.*, **32** [2] (2016) 129–133.
24. Ö. Keleş, R.E. Garcia, K.J. Bowman, "Stochastic failure of isotropic, brittle materials with uniform porosity", *Acta Mater.*, **61** [8] (2013) 2853–2862.